



Providing Choice & Value

Generic CT and MRI Contrast Agents



CONTACT REP

AJNR

The Role of Conventional MR Imaging Sequences in the Evaluation of Neurocysticercosis: Impact on Characterization of the Scolex and Lesion Burden

This information is current as of July 31, 2025.

L.T. Lucato, M.S. Guedes, J.R. Sato, L.A. Bacheschi, L.R. Machado and C.C. Leite

AJNR Am J Neuroradiol 2007, 28 (8) 1501-1504

doi: <https://doi.org/10.3174/ajnr.A0623>

<http://www.ajnr.org/content/28/8/1501>

ORIGINAL RESEARCH

L.T. Lucato
M.S. Guedes
J.R. Sato
L.A. Bacheschi
L.R. Machado
C.C. Leite

The Role of Conventional MR Imaging Sequences in the Evaluation of Neurocysticercosis: Impact on Characterization of the Scolex and Lesion Burden

BACKGROUND AND PURPOSE: There are few studies comparing the capacity of lesion detection of conventional MR imaging in neurocysticercosis (NCC). This study was designed to clarify its role in the evaluation of this disease, focusing on the total number of lesions identified and the characterization of the scolex.

MATERIALS AND METHODS: MR images from 115 patients were prospectively collected during a 3-year interval, including axial spin-echo (SE) T1-weighted; axial fast SE T2-weighted; axial fluid-attenuated inversion recovery (FLAIR); and gadolinium-enhanced axial, coronal, and sagittal SE T1-weighted sequences. They were compared regarding the potential for detection of NCC lesions and specifically of the scolex.

RESULTS: Comparing all sequences, we found that FLAIR images were more sensitive to the detection of the scolex ($P < .003$), whereas the last gadolinium-enhanced T1-weighted series (coronal or sagittal) identified the highest number of lesions ($P < .001$).

CONCLUSION: When dealing with NCC, optimal MR imaging protocols should include FLAIR images to obtain maximal rates of scolex detection. Special attention should be paid to the last gadolinium-enhanced sequence, which maximizes the quantification of lesion load.

Neurocysticercosis (NCC) is a clinical condition characterized by the parasitic involvement of the central nervous system (CNS) by the larval stage of the pork tapeworm *Taenia solium*. Humans become the intermediate host in the life cycle of the tapeworm by ingesting its eggs from contaminated water or uncooked food,¹ though recently the possibility of direct infection from a symptom-free carrier in the household has gained attention.² After the larvae are ingested, they lodge predominantly in the brain, muscles, and other soft tissues.³ When in the CNS, the larvae most frequently land in the parenchyma but not infrequently can lodge inside the ventricles and subarachnoid space, or a combination of these.³ Lesion location is critical in symptom development.^{3,4}

Diagnosis of NCC was greatly improved by the introduction of CT and MR imaging. These imaging techniques depict the location and number of lesions and their stages and the degree of inflammatory response to the parasite (perilesional edema and blood-brain barrier breakdown).^{4,5} MR imaging is considered the most accurate technique to accomplish this task; however, CT is more sensitive for detection of calcifications.⁵⁻⁸

Specifically from a diagnostic standpoint, from the many imaging findings of NCC, only the presence of cystic lesions demonstrating the scolex can be considered pathognomonic.⁹ The scolex is visualized as a bright nodule within the cyst, producing the so-called “hole-with-dot” imaging that is seen in some vesicular cysts located in the brain parenchyma, the subarachnoid space, or the ventricular system.¹⁰ Revised diag-

nostic criteria for NCC consider that cystic lesions showing the scolex on CT or MR imaging are an absolute criterion for diagnosis of the disease, allowing its definitive diagnosis.¹¹

Guidelines for treatment of NCC must be individualized in terms of number and location of lesions and must be based on the viability of the parasites within the nervous system.^{12,13} MR imaging covers all these aspects, representing a powerful tool to support therapeutic decisions. Because of the epidemiologic importance of NCC and the pivotal role of MR imaging in its evaluation,¹⁴ our purpose was to determine the optimal conventional MR imaging protocol when scanning patients with NCC by using a comparison of different sequences in a large cohort of subjects.

Materials and Methods

Patients

One hundred fifteen patients were initially referred by the neurology clinic of our institution. These patients were diagnosed with NCC on the basis of fulfillment of the “Definitive Diagnosis” category of the “Proposed Diagnostic Criteria for Neurocysticercosis,” produced during the International Symposium of Neurocysticercosis held at Lima, Peru, in 2000.¹¹ These patients were prospectively studied by using MR imaging between February 2000 and November 2003. Inclusion criterion was an interest in taking part in the study. Exclusion criteria were presence of any coexistent CNS pathology, especially infections, and also refusal to take part in the study. These patients, 42 women and 73 men, ranged in age from 4 to 64 years (mean age, 36 ± 11 years). The study was approved by the internal review board of our institution.

MR Imaging

MR imaging examinations were performed in 2 whole-body scanners operating at 0.5T (Gyrosan T5 II; Philips Medical Systems, Best, the Netherlands) and 1.5T (Signa Horizon LX; GE Healthcare, Milwaukee, Wis) with a standard quadrature head coil.

Received December 29, 2006; accepted after revision February 17, 2007.

From the Department of Radiology (L.T.L., M.S.G., C.C.L.), Clinics Hospital of the University of São Paulo, School of Medicine, São Paulo, Brazil; the Department of Neurology (L.A.B., L.R.M.), Clinics Hospital of the University of São Paulo, School of Medicine, São Paulo, Brazil; and the Institute of Mathematics and Statistics (J.R.S.), University of São Paulo, São Paulo, Brazil.

Please address correspondence to Leandro Tavares Lucato, Rua Professor Pedreira de Freitas, 372 ap. 101-E, Tatuapé-São Paulo-S.P.-Brazil CEP 03312-052; e-mail: ltlucato@uol.com.br

DOI 10.3174/ajnr.A0623

MR imaging protocol included the following sequences in all patients: axial spin-echo (SE) T1-weighted imaging (TR = 466–620 ms, TE = 12–14 ms, section thickness = 5–6 mm, matrix = 256 × 192, NEX = 2, FOV = 24 × 24 cm or 18 × 24 cm), axial fast spin-echo (FSE) T2-weighted imaging (TR = 4400–5700 ms, TE = 100–120 ms, echo-train length = 22–27, section thickness = 5–6 mm, matrix = 320 × 224 or 256 × 256, NEX = 2, FOV = 24 × 24 cm or 18 × 24 cm), axial fluid-attenuated inversion recovery (FLAIR) imaging (TR = 9600–11,002 ms, TE = 148–157 ms, inversion time = 2100–2300 ms, section thickness = 5–6 mm, matrix = 256 × 160, NEX = 1, FOV = 24 × 24 cm or 18 × 24 cm), and axial/sagittal/coronal SE T1-weighted imaging after injection of paramagnetic contrast (gadolinium) in the standard dose of 0.1 mmol/kg, with the same parameters as listed previously.

MR Imaging Analysis

Two experienced neuroradiologists (M.S.G. and C.C.L., with 10 and 12 years of experience in neurologic MR imaging, respectively) independently reviewed all the images. Only intracranial lesions were evaluated.

MR imaging examinations were grouped according to each of the sequences obtained by using hard copies as follows: axial SE T1 (T1), axial FSE T2 (T2), axial FLAIR (FLAIR), gadolinium-enhanced axial SE T1 (T1-Gd), and the last SE sequence of the 3 postcontrast series (coronal or sagittal). This sequence, the last gadolinium-enhanced (last T1-Gd) series, was acquired on average 8 minutes and 58 seconds after contrast injection.

Both observers analyzed 1 group of images at a time, independently, in different sessions, starting with the T1 and finishing with the last T1-Gd. There was a gap of at least a week between reading 1 group of images and the other. All images were evaluated with respect to lesion location (parenchymal, ventricular, or subarachnoid), total number of lesions detected (regardless of their stage), and the ability to depict the scolex (defined as a central or eccentric nodule in the wall of a cystic lesion).

Statistical Analysis

The total number of lesions detected by both examiners and also the total number of scolices were entered into the analysis.

Agreement between examiners in each of the MR images was analyzed by using paired Student *t* tests to investigate any kind of examiner bias and also by calculating the Spearman correlation coefficient (ρ) as a measure of coherence. Differences in the mean total number of lesions detected and in the mean total number of scolices depicted by the 5 MR sequences were assessed by using the Friedman test for more than 2 related samples. Post hoc comparisons were performed by using paired Student *t* tests. A $P < .05$ was considered a statistically significant difference. All *P* values were 2-tailed.

Results

Sixty-nine examinations (60%) were performed on the 0.5T magnet and 46 (40%) on the 1.5T. We evaluated a total of 115 examinations of patients with NCC; that means 675 sequences were analyzed (5 sequences per patient). There were no differences in the findings of our study when we analyzed separately examinations performed on 0.5T and 1.5T magnets (data not shown), so our option was to use the combined data from both.

Regarding the topography of the cysticercotic lesions on a patient basis, we found that 80 patients had exclusively parenchymal lesions (69.6%), 6 had ventricular lesions (5.2%), and 11 had subarachnoid lesions (9.6%). Eighteen patients (15.6%) had a combination of these.

Comparing both examiners for each MR sequence, we

Table 1: Mean total number of lesions detected in each MR sequence

	MR Imaging Sequence				
	T1	T2	FLAIR	Axial T1-Gd	Last (coronal or sagittal) T1-Gd
Mean total of lesions	10.95	14.91	14.58	14.84	18.97*

Note:—Mean total of lesions indicates pooled data of examiners A and B ($N = 115$).

* $P < .001$ for the global Friedman test and $P < .003$ for all post hoc comparisons.

found no significant differences between them regarding total number of lesions and scolices ($P = .07$ –.90, for all paired Student *t* tests). Moreover, there is a significant correlation between examiners ($\rho = 0.87$ –0.97, $P < .001$). Putting this in perspective, we accomplished comparative analysis among MR sequences by using pooled data from both observers. When analyzing the total number of lesions in any possible stage, we verified that the last T1-Gd series detected significantly more lesions than did FLAIR, T1-Gd, T1, and T2 series ($P < .001$ for the global Friedman test and $P < .003$ for all post hoc comparisons) (Table 1 and Fig 1). Evaluation of the number of scolices depicted within NCC cysts showed that a significantly higher number were identified on the FLAIR sequence compared with all other sequences ($P < .001$ for the global Friedman test and also for all post hoc tests) (Table 2 and Fig 2).

Discussion

NCC is considered the most common parasitic disease of the CNS.^{3,11,14} At the present time, this disease is endemic in several parts of the world, constituting a major public health issue, especially in some developing countries.^{6,7} Recently, immigration from endemic areas has increased the prevalence of this disease in developed countries.^{3,15} In Latin America, an estimated 75 million people live in areas where neurocysticercosis is endemic, and approximately 400,000 have symptomatic disease.¹⁶ Immunoassays for diagnosis of NCC include analysis of serum samples, which can be done by using enzyme-linked immunoelectrotransfer blot (EITB); CSF samples can be studied by using either EITB or enzyme-linked immunosorbent assay (ELISA).² Although EITB and ELISA have good specificity and sensitivity, their major limitation is related to patients with single intracranial cysticercus, in whom up to 40% can test negative for NCC.¹⁷ New diagnostic techniques in this field, such as mitochondrial DNA analysis, seem promising.¹⁸

Current strategies for diagnosis of NCC include neuroimaging studies,¹ because a wide variety of neurologic syndromes can be associated with the disease. MR imaging findings are protean, depending on the stage of evolution of the larvae and on the fact that a single patient can present lesions in different stages of the disease simultaneously.^{1,8} Four recognized stages are the following: vesicular, colloid vesicular, granular nodular, and nodular calcified.¹⁹

In the vesicular stage, the cysticercus is viable and elicits few inflammatory changes in the surrounding tissues. In this stage, the cyst has a thin wall and the cyst fluid has signal intensity similar to that of CSF in all sequences. In viable cysts, an eccentrically located mural nodule represents the scolex. No contrast enhancement or edema is seen.

In the colloidal stage, as an inflammatory reaction develops

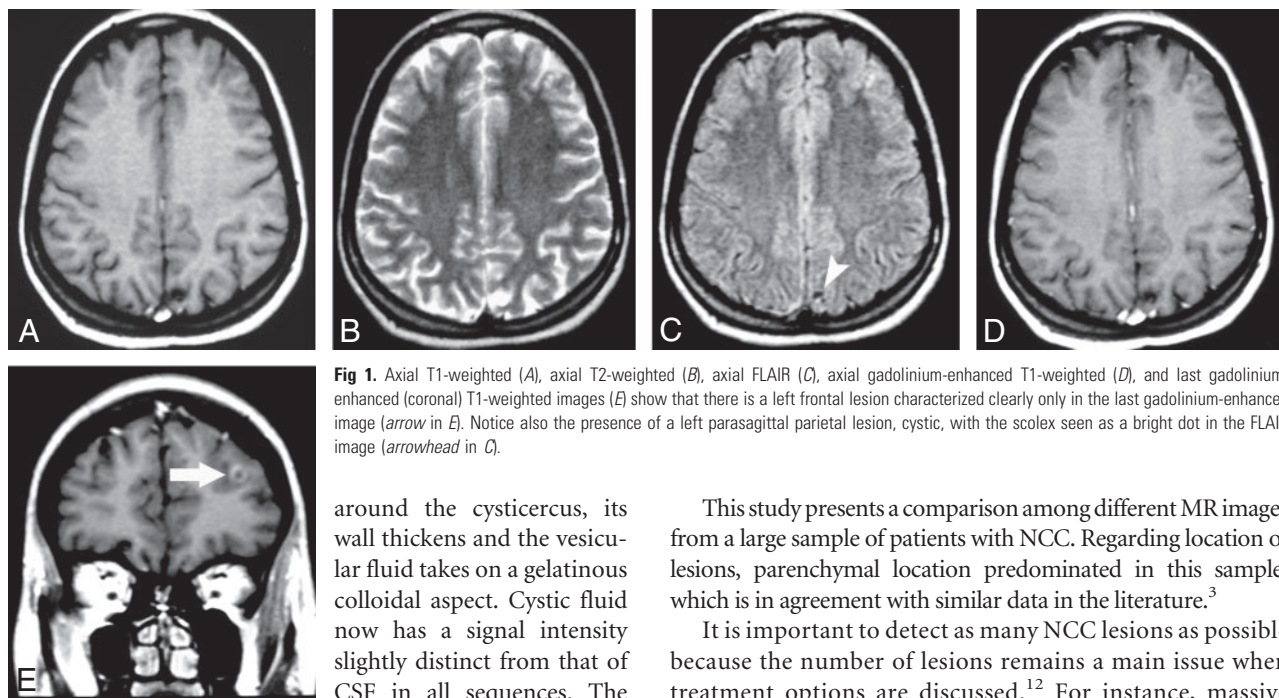


Fig 1. Axial T1-weighted (A), axial T2-weighted (B), axial FLAIR (C), axial gadolinium-enhanced T1-weighted (D), and last gadolinium-enhanced (coronal) T1-weighted images (E) show that there is a left frontal lesion characterized clearly only in the last gadolinium-enhanced image (arrow in E). Notice also the presence of a left parasagittal parietal lesion, cystic, with the scolex seen as a bright dot in the FLAIR image (arrowhead in C).

around the cysticercus, its wall thickens and the vesicular fluid takes on a gelatinous colloidal aspect. Cystic fluid now has a signal intensity slightly distinct from that of CSF in all sequences. The scolex begins to show signs of degeneration, and a gradual decrease in the size of the lesion is noticed. Contrast enhancement, usually peripheral, and perilesional edema are seen.

The parasite is already dead in the granular nodular stage, and the retracted lesion begins to mineralize. It becomes semi-solid as it is progressively replaced by granulomatous tissue. There is nodular or ring enhancement of the lesion, and edema is less extensive.^{1,4,5,7,8,20,21}

In the nodular calcified stage, the lesion is completely mineralized. These lesions appear as small nodules with hypointensity on T2-weighted and T2*-weighted images, better detected on CT studies. Some calcified lesions present persistent contrast enhancement on MR imaging^{1,4,5,22}; others may lead to active inflammation during therapy.¹³

Besides parenchymal NCC, the second most common site is ventricular,²³ especially in the fourth ventricle. The lesions are difficult to characterize in CT studies¹⁹ and can be missed even in MR imaging if one is not aware of the possibility of lesions in the ventricles. Signal intensity of the cyst is slightly different from that of CSF, usually without enhancement. Hydrocephalus is commonly detected and can be related to the clinical presentation of ventricular NCC, due to obstruction of CSF flow.²³

Subarachnoid NCC usually involves the basal cisterns and Sylvian fissures. These cysts have a signal intensity similar to that of CSF and usually do not enhance after the use of gadolinium. There is associated mass effect, causing local subarachnoid enlargement and a multiloculated appearance.²³ The scolex is rarely seen.¹⁹

Table 2: Mean number of scolices detected in each MR sequence

	MR Imaging Sequence				
	T1	T2	FLAIR	Axial T1-Gd	Last (coronal or sagittal) T1-Gd
Mean number of scolices	8.57	8.37	11.30*	9.23	9.33

Note:—Mean number of scolices indicates pooled data of examiners A and B ($N = 115$).
* $P < .001$ for the global Friedman test and also for all post hoc tests.

This study presents a comparison among different MR images from a large sample of patients with NCC. Regarding location of lesions, parenchymal location predominated in this sample, which is in agreement with similar data in the literature.³

It is important to detect as many NCC lesions as possible because the number of lesions remains a main issue when treatment options are discussed.¹² For instance, massive infections of the CNS are a potential contraindication to antiparasitic treatment. Considering this specific topic, we found that the last T1-Gd images demonstrated significantly more lesions than did all other sequences. This finding could be explained by an improvement in the detection of lesions in the degenerative phase (vesicular colloidal, granular nodular, and, in some cases, calcified nodular), which are prone to present enhancement²² related to an active inflammatory reaction elicited by the parasite in these stages.²⁴ Another factor probably related specifically to the superiority of the last T1-Gd series over the first gadolinium-enhanced sequence (T1-Gd) is the presence of time-dependent variations in image contrast. This is a well-known phenomenon affecting other CNS diseases.²⁵⁻²⁷

FLAIR images show the scolex as an eccentrically punctate bright signal intensity within the neurocysticercotic cysts.²⁰ A few studies addressed the advantages of using FLAIR images in the evaluation of NCC, but the results are scarce and related to the study of the disease as a whole.^{5,20,28,29}

The International Symposium in Lima, Peru in 2000 included the presence of the scolex in a given cystic lesion as an absolute diagnostic criterion of NCC, allowing unequivocal diagnosis of this disease.¹¹ It was demonstrated in the present study that FLAIR images disclosed more scolices than any other sequence, so we can speculate that in some specific settings, FLAIR can help to firm a final diagnosis of NCC. FLAIR was the one and only sequence to demonstrate the scolex in a significant number of patients, allowing the definitive diagnosis of NCC that was not possible using other sequences.

Our study has some limitations. NCC can sometimes present as tiny lesions, and the section thickness used in our protocol (5–6 mm) could potentially lead to an underestimation of the presence of these lesions, though this limitation was exactly the same for all sequences. We did not use a T2* sequence in our protocol, so the characterization of calcified lesions was impaired, though some of them could be occasionally identified in the T2 sequence and included in the total amount of lesions.

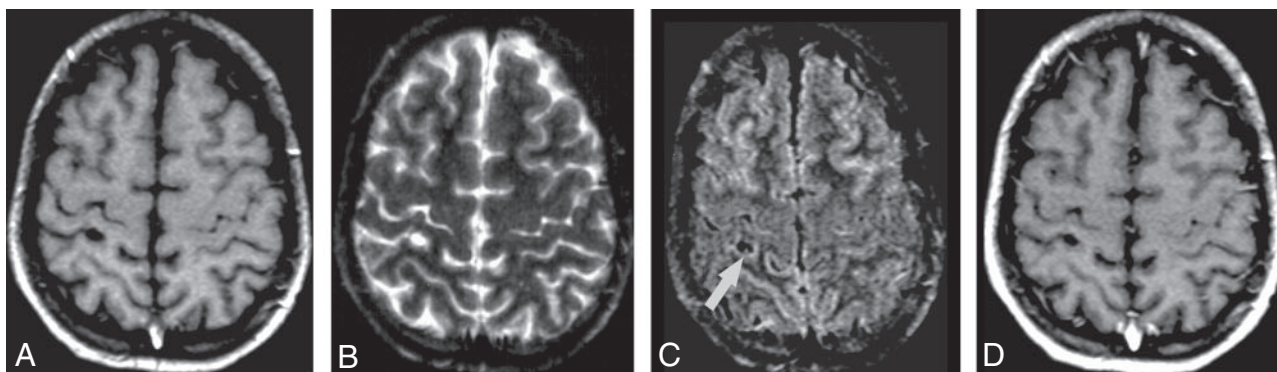


Fig 2. Axial T1-weighted (A), axial T2-weighted (B), axial FLAIR (C), and gadolinium-enhanced axial T1-weighted (D) images demonstrate that the ability to detect the scolex is present, in this case, only in the FLAIR image (arrow in C).

The fact that different magnetic fields were used for these examinations could also be a limitation, though this represents an issue mainly for calcifications, where detection relies on susceptibility effects (which are more prominent at 1.5T), and also for contrast enhancement, where conspicuity parallels roughly the magnetic field intensity. However, our findings were similar in both fields; besides, it is important to emphasize that these findings are also valid in low-field magnets, especially if we take into consideration that in developing countries, where NCC is endemic, they are quite common.

Because there were obvious differences among the types of images, the observers could not be blinded to the type of sequence they were evaluating. At least in part, one could speculate about some kind of learning effect leading to the superior performance of last T1-Gd, because it was systematically the last one to be analyzed. This probably has negligible influence because there was a reasonable time interval between readings in each group of images and the number of examinations to be analyzed was huge. Another point is that if there was some kind of learning effect, the number of lesions would probably increase from the first to the last sequence analyzed, which is something not appreciated in this study.

Future studies could address other important issues, such as the role of T2* images in the evaluation of this disease, compared specifically with CT to disclose calcifications, and also relatively new techniques such as diffusion-weighted images, if they somewhat impact the management of this disease.

Conclusion

Detection of a higher infection burden by the last T1-Gd series is an important aspect, which can have impact on therapeutic decisions, so it is necessary to pay close attention to this sequence. FLAIR images detect a significantly higher number of scolices than other sequences, which is helpful for the diagnosis of NCC.

References

- Carpio A, Escobar A, Hauser WA. Cysticercosis and epilepsy: a critical review. *Epilepsia* 1998;39:1025–40
- Garcia HH, Del Brutto OH. Neurocysticercosis: updated concepts about an old disease. *Lancet Neurol* 2005;4:653–61
- Wallin MT, Kurtzke JF. Neurocysticercosis in the United States: review of an important emerging infection. *Neurology* 2004;63:1559–64
- Zee CS, Go JL, Kim PE, et al. Imaging of neurocysticercosis. *Neuroimaging Clin N Am* 2000;10:391–407
- Garcia HH, Del Brutto OH. Imaging findings in neurocysticercosis. *Acta Trop* 2003;87:71–78
- Garcia HH, Gonzalez AE, Gilman RH. Diagnosis, treatment and control of *Taenia solium* cysticercosis. *Curr Opin Infect Dis* 2003;16:411–19
- Garcia HH, Gonzalez AE, Evans CA, et al. *Taenia solium* cysticercosis. *Lancet* 2003;362:547–56
- Castillo M. Imaging of neurocysticercosis. *Semin Roentgenol* 2004;39:465–73
- Dumas JL, Visy JM, Belin C, et al. Parenchymal neurocysticercosis: follow-up and staging by MRI. *Neuroradiology* 1997;39:12–18
- Suss RA, Maravilla KR, Thompson J. MR imaging of intracranial cysticercosis: comparison with CT and anatomopathologic features. *AJNR Am J Neuroradiol* 1986;7:235–42
- Del Brutto OH, Rajshekhar V, White AC Jr, et al. Proposed diagnostic criteria for neurocysticercosis. *Neurology* 2001;57:177–83
- Garcia HH, Evans CA, Nash TE, et al. Current consensus guidelines for treatment of neurocysticercosis. *Clin Microbiol Rev* 2002;15:747–56
- Poeschl P, Janzen A, Schuierer G, et al. Calcified neurocysticercosis lesions trigger symptomatic inflammation during antiparasitic therapy. *AJNR Am J Neuroradiol* 2006;27:653–55
- Yancey LS, Diaz-Marchan PJ, White AC. Cysticercosis: recent advances in diagnosis and management of neurocysticercosis. *Curr Infect Dis Rep* 2005;7:39–47
- Flisser A, Sarti E, Lightowlers M, et al. Neurocysticercosis: regional status, epidemiology, impact and control measures in the Americas. *Acta Trop* 2003;87:43–51
- Bern C, Garcia HH, Evans C, et al. Magnitude of the disease burden from neurocysticercosis in a developing country. *Clin Infect Dis* 1999;29:1203–09
- Prabhakaran V, Rajshekhar V, Murrell KD, et al. *Taenia solium* metacystode glycoproteins as diagnostic antigens for solitary cysticercosis granuloma in Indian patients. *Trans R Soc Trop Med Hyg* 2004;98:478–84
- Ishikawa E, Komatsu Y, Kikuchi K, et al. Neurocysticercosis as solitary parenchymal lesion confirmed by mitochondrial deoxyribonucleic acid sequence analysis. *Neurol Med Chir (Tokyo)* 2007;47:40–44
- do Amaral LL, Ferreira RM, da Rocha AJ, et al. Neurocysticercosis: evaluation with advanced magnetic resonance techniques and atypical forms. *Top Magn Reson Imaging* 2005;16:127–44
- Sander HW, Castro C. Images in clinical medicine: neurocysticercosis. *N Engl J Med* 2004;350:266
- Silbert PL, Gubbay SS, Khangure M. Distinctive MRI findings in a case of neurocysticercosis. *Med J Aust* 1993;159:185–86
- Sheth TN, Pillon L, Keystone J, et al. Persistent MR contrast enhancement of calcified neurocysticercosis lesions. *AJNR Am J Neuroradiol* 1998;19:79–82
- Amaral L, Maschietto M, Maschietto R, et al. Unusual manifestations of neurocysticercosis in MR imaging: analysis of 172 cases. *Arq Neuropsiquiatr* 2003; 61:533–41. Epub 2003 Sep 16
- Chang KH, Lee JH, Han MH, et al. The role of contrast-enhanced MR imaging in the diagnosis of neurocysticercosis. *AJNR Am J Neuroradiol* 1991;12:509–12
- Schorner W, Laniado M, Niendorf HP, et al. Time-dependent changes in image contrast in brain tumors after gadolinium-DTPA. *AJNR Am J Neuroradiol* 1986;7:1013–20
- Yuh WT, Tali ET, Nguyen HD, et al. The effect of contrast dose, imaging time, and lesion size in the MR detection of intracerebral metastasis. *AJNR Am J Neuroradiol* 1995;16:373–80
- Runge VM, Wells JW, Williams NM, et al. The use of gadolinium-BOPTA on magnetic resonance imaging in brain infection. *Invest Radiol* 1996;31:294–99
- Singh S, Gibikote SV, Shyamkumar NK. Isolated fourth ventricular cysticercosis: MR imaging in 4 cases with short literature review. *Neurol India* 2003;51:394–96
- Tsuchiya K, Inaoka S, Mizutani Y, et al. Fast fluid-attenuated inversion-recovery MR of intracranial infections. *AJNR Am J Neuroradiol* 1997;18:909–13